



69th Conference of the Italian Thermal Machines Engineering Association, ATI2014

Transient analysis of a solar domestic hot water system using two different solvers

Luigi Mongibello^{a,*}, Nicola Bianco^b, Martina Caliano^{b,c}, Adriano de Luca^d, Giorgio Graditi^a

^a ENEA Italian National Agency for New Technologies, Energy and Sustainable Economic Development - Portici RC, 80055 Portici (NA), Italy

^b Dipartimento di Ingegneria Industriale (DII) – Università degli Studi Federico II, 80125 Napoli, Italy

^c Dipartimento di Ingegneria Meccanica, Energetica e Gestionale (DIMEG) – Università della Calabria, 87036 Cosenza, Italy

^d Dipartimento di Ingegneria Industriale (DIIN) – Università degli Studi di Salerno, 84084 Fisciano (SA), Italy

Abstract

In the present work the unsteady numerical simulation of a solar domestic hot water (DHW) system composed of two flat plate collectors, a water tank for heat storage, and a coil heat exchanger is addressed. The simulations have been performed using two different solvers, namely a home-made code written in Matlab, and TRNSYS 17. In the first part of the paper, the analytical models used in the Matlab code, and the TRNSYS case are reported in detail. Successively, the results of the simulations realized by means of the two solvers are presented and compared.

© 2015 The Authors. Published by Elsevier Ltd. This is an open access article under the CC BY-NC-ND license

(<http://creativecommons.org/licenses/by-nc-nd/4.0/>).

Peer-review under responsibility of the Scientific Committee of ATI 2014

Keywords: analytical models; one-day simulation; experimental input data; home-made solver; TRNSYS 17

1. Introduction

The use of solar thermal collectors for the production of domestic hot water (DHW) has experienced a considerable worldwide growth in the last years due essentially to its cost effectiveness.

In recent years, several studies have focused on transient mathematical models of solar DHW systems. Among these, the most regarded references for the present work are represented by the papers of Rodriguez-Hidalgo *et al.* [1,2], who developed and validated experimentally a transient model in order to achieve the design criteria of solar

* Corresponding author. Tel.: +39-081-7723584; fax: +39-081-7723344.

E-mail address: luigi.mongibello@enea.it

DHW plants under daily transient conditions.

This paper is focused on the numerical simulation of a solar DHW system composed of two non-concentrating flat plate collectors connected in series, a vertical cylindrical water tank for heat storage, and a coil heat exchanger immersed into the water tank. Fig. 1 shows a sketch of the present system. The numerical simulations of the system performances have been realized using a home-made numerical code written in Matlab, and the commercial software TRNSYS 17. The aim of this work is to present in detail the characteristics of the home-made solver, and to demonstrate its effectiveness in simulating the basic operation of a solar DHW system by comparing its results with those of the TRNSYS solver.

In the first part of the paper, the analytical models, the numerical schemes and algorithms used in the Matlab code, and the TRNSYS case are reported in detail. Successively, the results of the simulations realized by means of the two solvers and using as input data experimental values of the irradiance, ambient temperature and wind velocity are presented and compared.

Nomenclature

A	surface area (m^2)
c_p	specific heat ($\text{J kg}^{-1} \text{K}^{-1}$)
D	diameter (m)
\bar{h}	mean convective heat transfer coefficient ($\text{W m}^{-2} \text{K}^{-1}$)
<i>INERZIA</i>	thermal inertia (W)
k	thermal conductivity ($\text{W m}^{-1} \text{K}^{-1}$)
L	thickness (m)
N	number of isothermal nodes
Q	heat power (W)
r	radius (m)
R	thermal resistance (K W^{-1})
T	temperature (K)
t	time (s)
\dot{V}	flow rate ($\text{m}^3 \text{s}^{-1}$)
V	volume (m^3)
v	wind velocity (m s^{-1})

Greek symbols

ε	emissivity
ρ	density (kg m^{-3})
σ	Stefan-Boltzmann constant ($\text{W m}^{-2} \text{K}^{-4}$)

Subscript

<i>abs</i>	absorber plate
<i>absorbed</i>	absorbed heat power
<i>air</i>	ambient air
<i>amb</i>	ambient
<i>box</i>	box back surface of flat plate collector
<i>cd</i>	convective at the collector downwards
<i>cint</i>	convective in the air enclosure of the collector
<i>co</i>	collector
<i>coil</i>	heat exchanger coil
<i>cond</i>	conductive
<i>conv</i>	convective
<i>cup</i>	convective at the collector upwards

<i>D</i>	diffuse
<i>d</i>	downwards
<i>enc</i>	air enclosure
<i>ext</i>	external
<i>glass</i>	glass cover of the flat plate collector
<i>in</i>	inner
<i>ins</i>	insulation
<i>int</i>	internal
<i>k</i>	summation index
<i>layer</i>	layer of the tank
<i>nod</i>	discretization node
<i>out</i>	outer
<i>rad</i>	radiation
<i>serp</i>	collector serpentine
<i>sky</i>	sky
<i>solar</i>	solar irradiance
<i>tank</i>	heat storage tank
<i>tot</i>	total
<i>up</i>	upwards
<i>useful</i>	useful power
<i>w</i>	water
<i>Abbreviations</i>	
DHW	domestic hot water
HTF	heat transfer fluid
HX	heat exchanger

2. Solar DHW system components models

2.1. Solar collectors model

The solar thermal collectors considered in the present study are the commercial flat-plate Vitosol 100 w2.5 by Viessmann Werke GmbH and Co KG®. Table 1 reports the main data relative to each collector. They have been considered installed in Portici (Italy), oriented to south and with a slope of 30°. A solution of water and propylene glycol (30%) has been considered as HTF.

A zero-dimensional analytical model has been developed to evaluate the time-variable temperature of each collectors component, as well as the temperature of the HTF at the exit sections of the collectors serpentine.

Fig. 2 shows a sketch of a cross section of the single collector and the equivalent thermal circuit relative to the lumped-element model that has been used to perform the energy balance.

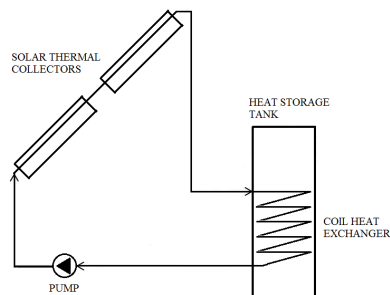


Fig. 1. Sketch of the solar DHW system.

With reference to fig. 2, for each collector the following relations hold:

$$R_{ins} Q_d = T_{abs} - T_{box} \quad (1)$$

$$R_{cd} Q_d = T_{box} - T_{amb} \quad (2)$$

$$R_{int} Q_{up} = T_{abs} - T_{glass} \quad (3)$$

$$R_{cup} Q_{cup} = T_{glass} - T_{amb} \quad (4)$$

$$R_{rad_ext} Q_{rad} = T_{glass} - T_{sky} \quad (5)$$

$$Q_{up} = Q_{solar} - Q_d - Q_{useful} - INERZIA \quad (6)$$

$$Q_{solar} = Q_{co} A_{co} \quad (7)$$

$$Q_{useful} = \dot{V}_{HTF} \rho_{HTF} c_{p_{HTF}} (T_{HTF_out} - T_{HTF_in}) \quad (8)$$

$$R_{tot_HTF} Q_{absorbed_HTF} = \left(T_{abs} - \frac{(T_{HTF_out} + T_{HTF_in})}{2} \right) \quad (9)$$

$$Q_{absorbed_HTF} - Q_{useful} = V_{HTF} \rho_{HTF} c_{p_{HTF}} \frac{dT_{HTF}}{dt} \quad (9bis)$$

$$Q_{cup} = Q_{up} - Q_{rad} \quad (10)$$

$$INERZIA = \sum_k V_k \rho_k c_{p_k} \frac{dT_k}{dt} \quad (11)$$

The insulation thermal resistance is given by:

$$R_{ins} = \frac{L_{ins}}{A_{ins} k_{ins}} \quad (12)$$

Table 1. Collector data

Collector width (m)	2.39
Collector length (m)	1.14
Absorber area (m ²)	2.50
Glass cover thickness (m)	4.0·10 ⁻³
Inner air layer thickness (m)	2.6·10 ⁻²
Absorber sheet thickness (m) - (Cu)	2.5·10 ⁻⁴
Outer serpentine diameter (m) - (Cu)	1.0·10 ⁻²
Inner serpentine diameter (m) - (Cu)	8.0·10 ⁻³
Insulation thickness (m) - mineral fiber	5.0·10 ⁻²
Box back cover thickness (m) - (Al)	2.0·10 ⁻³
Glass emissivity	0.85
Glass transmittance	0.90
Absorber absorptance	0.94

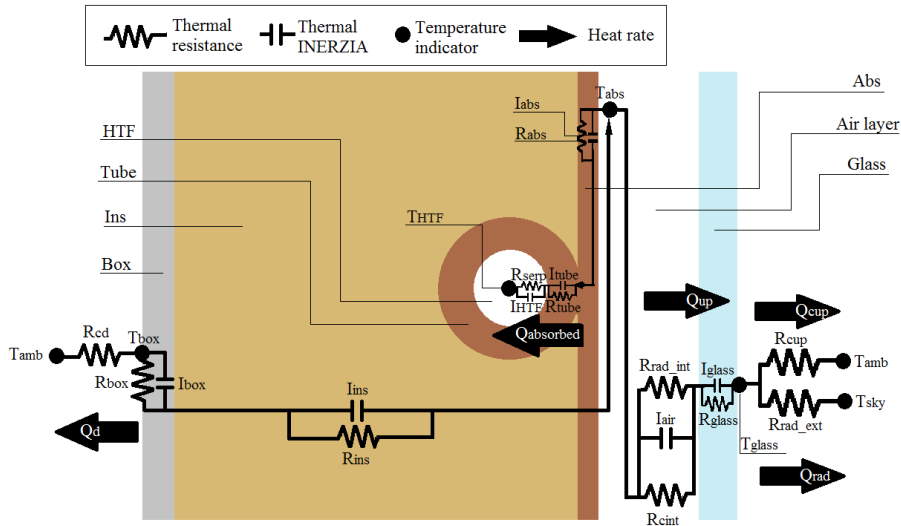


Fig. 2. Cross section and equivalent thermal circuit of the collector.

The thermal resistance relative to the internal air layer has been evaluated considering the parallel contributions of the radiative and the convective heat transfer mechanisms, and it is given by:

$$R_{int} = (R_{rad_int}^{-1} + R_{cint}^{-1})^{-1} \tag{13}$$

where R_{rad_int} is evaluated as:

$$R_{rad_int} = \frac{\left(\frac{1}{\epsilon_{glass}} + \frac{1}{\epsilon_{abs}} - 1 \right)}{\sigma A_{co} (T_{glass}^2 + T_{abs}^2) (T_{glass} + T_{abs})} \tag{14}$$

The internal convective thermal resistance is given by:

$$R_{cint} = \frac{1}{h_{cint} A_{cint}} \tag{15}$$

where the convective heat transfer coefficient is evaluated by using the Hollad correlation [3].

The external radiative thermal resistance is given by:

$$R_{rad_ext} = \frac{1}{\sigma \epsilon_{glass} A_{co} (T_{glass}^2 + T_{sky}^2) (T_{glass} + T_{sky})} \tag{16}$$

The convective thermal resistance at the box back surface is given by:

$$R_{cd} = \frac{1}{h_{cd} A_{cd}} \tag{17}$$

The mean convective heat transfer coefficient at the back box surface in equation (17) is evaluated using the correlation of Watmuff *et al.* [4]:

$$\bar{h}_{cd} = 2.8 + 3.0v \quad (18)$$

The convective thermal resistance at the glass cover is evaluated in a similar way. In equation (5), T_{sky} represents the so called “sky temperature” evaluated as in [5]:

$$T_{sky} = 0.0552T_{amb}^{1/5} \quad (19)$$

In equation (7), Q_{co} represents the fraction of the irradiance that is absorbed by the absorber plate, and it has been calculated by means of the HDKR model [6-8].

The calculation of the thermal resistance relative to the heat transfer between the HTF flowing through the serpentine and the absorber has been accomplished considering only the contribution of the convective heat transfer. It is given by:

$$R_{tot_HTF} = \frac{1}{h_{serp} A_{int_serp}} \quad (20)$$

where the convective heat transfer coefficient is evaluated by means of the classical Nusselt number correlation for thermally fully developed laminar flow, being the Reynolds number lower than 2300.

At each time-step, the system of equations (1-11) is solved implicitly. The input temperature of the HTF at the inlet of the first collector is taken from the coil heat exchanger simulation, while the HTF temperature at the inlet of the second collector is considered equal to the HTF temperature at the outlet of the first collector. The model outputs are the time-variable temperatures of all the collector components, and the time-variable HTF temperature at the exit of the collectors serpentes.

2.2. Immersed coil heat exchanger model

A transient one-dimensional model has been adopted for the evaluation of the temperature field of the HTF flowing through the immersed coil heat exchanger (HX). The data of the coil heat exchanger that has been considered in the present study are reported in table 2.

The heat exchanger has been divided in a predetermined number of isothermal nodes N_{coil} representing tube sections having the same volume. For each node, the energy balance equation is given by:

$$\rho_{HTF} V_{nod} c_{p_{HTF}} \frac{dT_{HTF}}{dt} = \frac{(T_{tank} - T_{HTF})}{R_{coil}} + \rho_{HTF} \dot{V}_{HTF} c_{p_{HTF}} (T_{HTF_in} - T_{HTF_out}) \quad (21)$$

The thermal resistance between the HTF in the coil heat exchanger and the water in the heat storage tank is given by:

$$R_{coil} = R_{conv_int} + R_{conv_ext} + R_{cond} \quad (22)$$

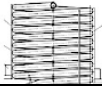
where

$$R_{conv_int} = \frac{1}{h_{int_coil} A_{int_coil}} \quad (23)$$

The mean internal convective heat transfer coefficient in equation (23) is evaluated using the Gnielinski's correlation for coiled tube heat exchanger [9] for the Nusselt number.

Table 2. Immersed coil heat exchanger data.

Thermal conductivity (W/m/K)	15.0
Inner diameter (m)	$2.37 \cdot 10^{-2}$
Outer diameter (m)	$2.69 \cdot 10^{-2}$
Helix diameter (m)	$49.0 \cdot 10^{-2}$
Helix height (m)	$47.5 \cdot 10^{-2}$
Helix length (m)	20.45
Helix outer area (m ²)	1.69



The external convective thermal resistance has been evaluated as:

$$R_{conv_ext} = \frac{1}{h_{ext_coil} A_{ext_coil}} \quad (24)$$

The mean external convective heat transfer coefficient in equation (24) is evaluated using the Morgan's correlation for natural convection for horizontal cylinders [10] for the Nusselt number.

The conductive thermal resistance of the coil has been neglected, because its order of magnitude is much lower than the internal and external convective thermal resistances.

For each time-step and for each node, equation (21) is solved using the implicit Euler method. The input data for the simulation are represented by the HTF temperature at the inlet section, that has been considered equal to the HTF temperature at the outlet of the second collector, and by the temperature field of water inside the storage tank.

The output of the model is represented by the HTF outlet temperature relative to each node.

2.3. Heat storage tank model

A vertical cylindrical heat storage tank has been considered in the present study. The tank volume is 0.4 m^3 , and the tank height and diameter are 1.50 m and 0.58m, respectively. The immersed coil heat exchanger inlet has been located on the tank lateral wall at an height of 0.975 m from the tank bottom, while the outlet at 0.5 m. No hot water loading from the tank have been simulated. Hence, forced convection wasn't modelled.

In the present 1D model the water is considered divided into N_{tank} isothermal node representing water layers of equal volume.

The energy balance for each node is written as:

$$\rho_w V_w c_{p_w} \frac{dT_w}{dt} = \frac{(T_{HTF} - T_w)}{R_{coil}} + Q_{cond} - \frac{(T_w - T_{amb})}{R_{tank}} \quad (25)$$

The thermal resistance relative to each layer of the storage wall has been evaluated as:

$$R_{tank} = R_{conv_int} + R_{cond} + R_{conv_ext} \quad (26)$$

where

$$R_{conv_int} = \frac{1}{h_{int_tank} A_{int_tank}} \quad (27)$$

The mean convective heat transfer coefficient relative to the inner tank wall in equation (31) is evaluated using the Nusselt number correlation for free convection relative to vertical flat plate.

The conductive thermal resistance relative to the tank wall has been evaluated as:

$$R_{cond} = \frac{\ln\left(\frac{r_{out_tank}}{r_{in_tank}}\right)}{2\pi k_{ins} \Delta_{layer}} \quad (28)$$

It has been assumed that the tank thickness is equal to the insulation thickness (0.05m, expanded polyurethane), namely that the conductive thermal resistance relative to the tank steel wall is negligible.

The convective thermal resistance relative to the external tank wall has been evaluated as:

$$R_{conv_ext} = \frac{1}{h_{ext_tank} A_{ext_tank}} \quad (29)$$

For each time-step and for each node, the energy balance equations system composed of equation (25) written for all nodes is solved using the implicit Euler method. The empirical reversion-elimination algorithm [11,12] has been adopted in order to include the effects of natural convection heat transfer between the water layers at different heights on the thermal stratification inside the tank. The input data for the heat storage tank model are represented by the ambient temperature and the temperatures field of the HTF.

2.4. Components coupling

The numerical simulation of the entire solar DHW system has been performed by means of a home-made code written in Matlab. The coupling between the system components has been dealt with an iterative approach. At each time step, the collectors simulation is performed first by using as input temperature at the HTF inlet section of the first collector the HTF temperature at the exit of the coil heat exchanger relative to the previous time-step. Then, the coil heat exchanger is simulated using as HTF inlet temperature the HTF temperature at the second collector exit section resulting from the collectors simulation previously made, and the tank water temperatures field relative to the previous time step. Successively, the tank is simulated using the updated temperatures of the HTF inside the coil heat exchanger. Then the process restart from the collectors simulation using the updated temperatures and go on till convergence.

3. TRNSYS simulation

The present solar DHW system has also been simulated using the commercial software TRNSYS 17, which is a complete and extensible simulation environment for the transient simulation of systems. Fig. 4 shows the TRNSYS components that have been used in the simulation. In particular, the Type 73 has been used for the collectors. This type performs the calculation of the energy gain relative to the series of flat plate collectors on the basis of the Hotter-Whillier equation, and it evaluates the thermal losses of the collectors by means of an overall loss coefficient depending on the collectors design and operating conditions [13]. The Type 534 has been used for the system composed of the heat storage tank and the immersed coiled tube heat exchanger. This type permits to specify the precise position of the heat exchanger inlet and outlet on the tank, and the portion of the heat exchanger length immersed in each tank node.

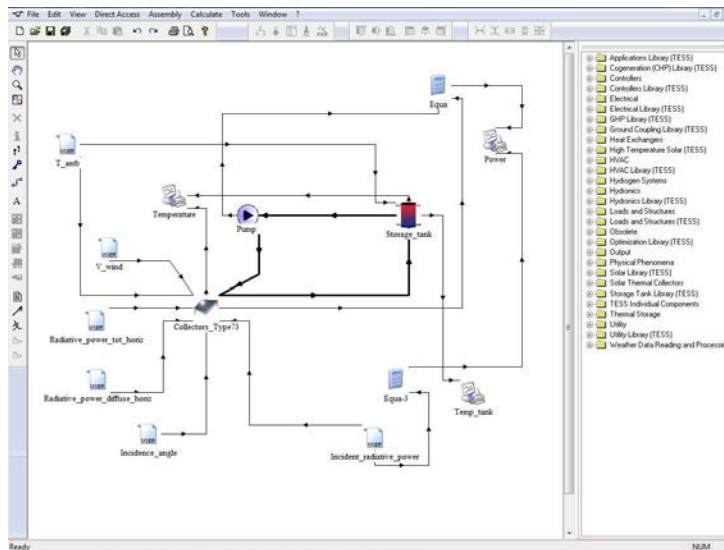


Fig. 3. TRNSYS 17 diagram of solar DHW simulation.

4. Simulations results

In this section, the results of the one-day simulation of the solar DHW system performed using both the Matlab code and the TRNSYS software are shown. The following results have been obtained for both solvers considering the HX and the heat storage tank discretized into 16 and 50 isothermal nodes, respectively. However, grid independence of results has been assured. The time-varying irradiance, ambient temperature and wind velocity, representing the input data for the whole model, have been measured at the ENEA Portici RC. Fig. 4 shows the irradiance, ambient temperature and wind velocity experimental profiles. The HTF flow rate has been set equal to $3 \cdot 10^{-5} \text{ m}^3/\text{s}$, and a time-step of 60 s has been used. The initial temperatures of the collectors components have been set equal to the ambient temperature at midnight, while the initial temperatures of the water in the tank and of the HTF in the heat exchanger have been considered equal to 18°C .

Fig. 5 shows the HTF temperatures at the heat exchanger inlet and outlet, the mean temperature of the tank water resulting from the implementation of the two solvers. Since the heat losses through the piping system have been neglected, the HTF temperature at the heat exchanger inlet represents also the HTF temperature at the second collector outlet, while the HTF temperature at the heat exchanger outlet represents also the HTF temperature at the first collector inlet.

As expected, the HTF and water temperatures increase considerably after the sunrise, and the maximum value of the HTF temperature at the exit of the second collector is reached at about 3:00 pm. It can be noticed that at about 5:00 pm the HTF temperatures at the heat exchanger inlet and outlet reach the same value. Afterwards, till midnight, the HTF temperature at the outlet is higher than the one at the inlet, and the tank water mean temperature decreases.

In practice, from that point to midnight the heat is not transferred from the collectors to the water in the tank, but it happens the contrary. This can be also seen in figg. 6 and 7, showing the time evolution of the water temperature at different tank nodes (node 1 is the at the tank bottom), and the useful power relative to the solar collectors together with the total radiative power incident on the collectors absorbers, respectively. Indeed, from about 5:00 pm to midnight the temperature profiles relative to the tank nodes 30 and 50 present a decreasing behaviour, and the total useful power relative to collectors becomes negative.

As to the comparison between the results relative to the two different solvers, it can be noticed that they produce very similar temperature profiles, with the maximum relative difference between the analogous temperature profiles never exceeding 10% in fig. 5, and 7% in fig. 6. Moreover, in fig. 7 it can be seen that also the useful power profiles produced by the two different solvers are in good accordance.

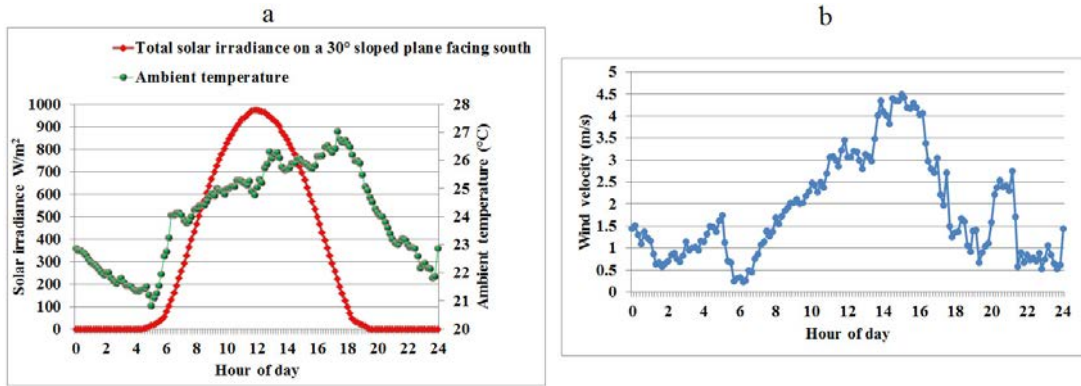


Fig. 4. Experimental data measured at ENEA Portici RC on July 3, 2013: (a) irradiance and ambient temperature; (b) wind velocity.

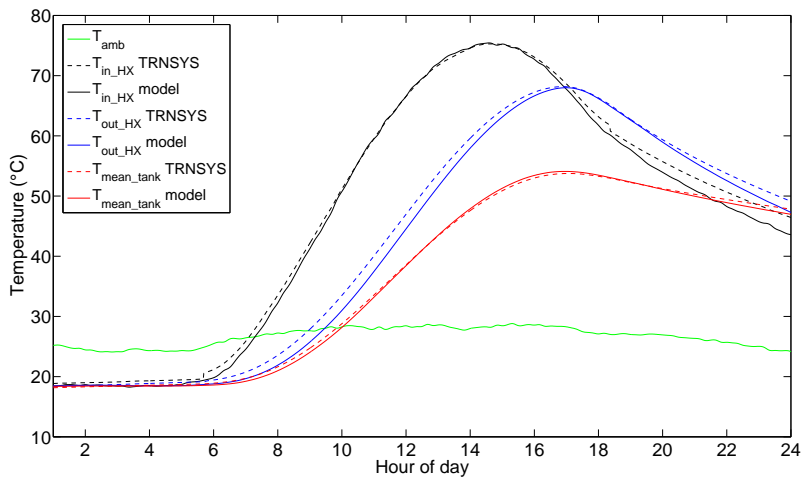


Fig. 5. Temperatures at the heat exchanger inlet and outlet, water tank mean temperature and ambient temperature.

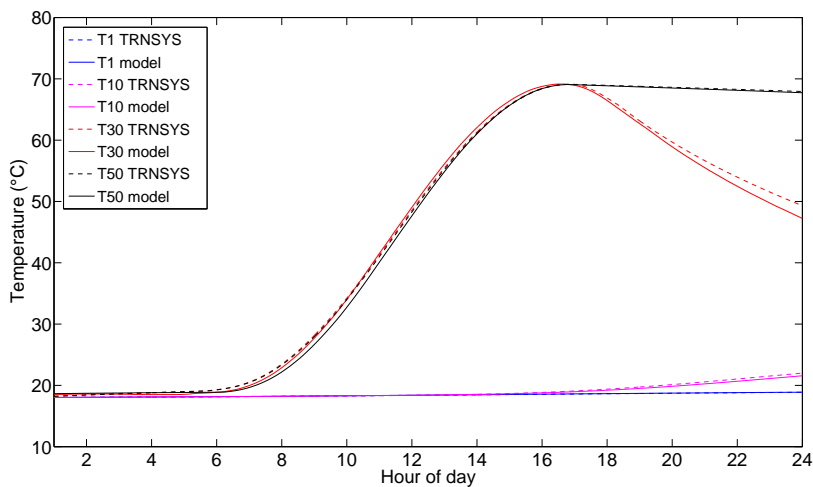


Fig. 6. Water temperature at different tank nodes (node 1 is the at the tank bottom).

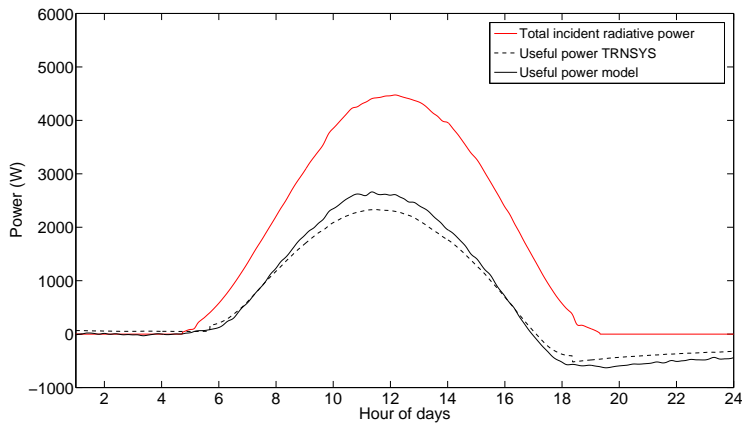


Fig. 7. Total incident radiative power on the absorbers, and useful power relative to the collectors.

5. Conclusions

In this paper the numerical simulation of the basic performances of a solar DHW system composed of two non-concentrating flat plate solar collectors, a vertical cylindrical water tank for heat storage, and an immersed coil heat exchanger has been addressed.

The simulations have been performed using two different solvers, namely a home-made numerical code written in Matlab, and the commercial software TRNSYS 17. The mathematical models and the numerical schemes implemented in the Matlab home-made code have been described in detail, and the features of the TRNSYS simulation have been reported as well.

The results of the simulations realized using as input data the irradiance, the ambient temperature and the wind velocity measured at the ENEA Portici Research Center in a summer day have been presented and discussed. The realistic temperatures and useful power trends, and the good accordance between the results obtained by means of the two different solvers demonstrate the effectiveness of the home-made tool.

References

- [1] Rodriguez-Hidalgo MC, Rodriguez-Aumente PA, Lecuona A, Gutierrez-Urueta GL, Ventas R. Flat plate thermal solar collector efficiency: Transient behaviour under working conditions. Part I. Model description and experimental validation. *Applied Thermal Engineering* 2011;31:2394-404.
- [2] Rodriguez-Hidalgo MC, Rodriguez-Aumente PA, Lecuona A, Gutierrez-Urueta GL, Ventas R. Flat plate thermal solar collector efficiency: Transient behaviour under working conditions. Part II: Model application and design contributions. *Applied Thermal Engineering* 2011;31:2385-393.
- [3] Hollands KGT, Unny TE, Raithby GD, Konicek L. Free Convective Heat Transfer across Inclined Air Layers. *J. Heat Transfer* 1976;98:189-93.
- [4] Watmuff JH, Charters WWS, Proctor D. Solar and wind induced external coefficients for solar collectors. *Comptes. Int. Rev. d'Hellio Tech.* 1977.p.56.
- [5] Ashrae HVAC Application Handbook 1999.
- [6] Hay JE, Davies JA. Calculation of the solar radiation incident on an inclined surface. *Proc. First Canadian Solar Radiation Data Workshop* 1980.
- [7] Klucher TM. Evaluating models to predict insolation on tilted surfaces. *Solar Energy* 1979;23:111-114.
- [8] Reindl DT, Beckman WA, Duffie JA. Evaluation of hourly tilted surface radiation models. *Solar Energy*, 1990;45:9-17.
- [9] Gnielinski Y. Heat transfer and pressure drop in helically coiled tubes. *Heat Transfer* 1986.p. 2847-854.
- [10] Morgan, V.T., The overall convective heat transfer from smooth circular cylinders, *Adv Heat Transfer*, 1975, 11, pp. 199-264.
- [11] Mather DW, Hollands KGT, Wright JL. Single- and Multi-Tank energy storage for solar heating systems: Fundamentals. *Solar Energy* 2002;73:3-13.
- [12] Newton BJ, Schmid M, Mitchell JW, Beckman WA. Storage tank models. *Proceedings of ASME/JSME/JSES International Solar Energy Conference 1995, Maui, Hawaii.*
- [13] Klein SA, Calculation of flat-plate collector loss coefficients, *Solar Energy*,1975,17,79-80.